



# Integrated analysis of the lncRNA-miRNA-mRNA ceRNA network in nasopharyngeal carcinoma

Yang Li<sup>1</sup>, Hui Zhong<sup>2</sup>, Lan Luo<sup>3</sup>, Mei Gan<sup>3</sup>, Li Liang<sup>3</sup>, Lilin Que<sup>3</sup>, Shaojun Zheng<sup>4</sup>, Jinghua Zhong<sup>5</sup>, Leifeng Liang<sup>3</sup>

<sup>1</sup>Department of Pharmacy, The Sixth Affiliated Hospital of Guangxi Medical University, The First People's Hospital of Yulin, Yulin, China;

<sup>2</sup>Department of Otolaryngology Head and Neck Surgery, The Sixth Affiliated Hospital of Guangxi Medical University, The First People's Hospital of Yulin, Yulin, China; <sup>3</sup>Department of Oncology, The Sixth Affiliated Hospital of Guangxi Medical University, The First People's Hospital of Yulin, Yulin, China; <sup>4</sup>Guangdong Provincial Key Laboratory of Infectious Diseases and Molecular Immunopathology, Institute of Oncologic Pathology, Cancer Research Center, Shantou University Medical College, Shantou, China; <sup>5</sup>Department of Oncology, The First Affiliated Hospital of Gannan Medical University, Ganzhou, China

**Contributions:** (I) Conception and design: Y Li, H Zhong, Leifeng Liang; (II) Administrative support: None; (III) Provision of study materials or patients: Leifeng Liang; (IV) Collection and assembly of data: L Luo, Li Liang, L Que, S Zheng; (V) Data analysis and interpretation: M Gan, Li Liang, J Zhong; (VI) Manuscript writing: All authors; (VII) Final approval of manuscript: All authors.

**Correspondence to:** Leifeng Liang, PhD. Department of Oncology, The Sixth Affiliated Hospital of Guangxi Medical University, The First People's Hospital of Yulin, 495 Education Middle Road, Yulin 537000, China. Email: liangleifeng@stu.gxmu.edu.cn.

**Background:** Nasopharyngeal carcinoma (NPC) is particularly prevalent in East and Southeast Asia. Competing endogenous RNA (ceRNA) networks are known to play an essential role in the emergence of various diseases, including cancer. Building a network of protein-protein interactions (PPIs) and ceRNAs can facilitate the detection of potential connections between messenger RNAs (mRNAs) and various non-coding RNAs. However, the precise role of ceRNA networks in NPC has not been examined in detail. Therefore, the primary aim of the present study was to characterize a ceRNA network for NPC.

**Methods:** Datasets of microRNA (miRNA), long non-coding RNA (lncRNA), and mRNA microarrays were downloaded from the Gene Expression Omnibus (GEO) database. Data were standardized and differentially expressed genes (DEGs) were screened using the limma package. The ClusterProfiler software suite was used to perform enrichment analysis of differentially expressed mRNAs using Gene Ontology (GO), Kyoto Encyclopedia of Genes and Genomes (KEGG), and gene set enrichment analysis (GSEA) techniques.

**Results:** A total of 160 lncRNAs, 8 miRNAs, and 147 mRNAs were differentially expressed in NPC samples. A ceRNA network was constructed using four lncRNAs, five miRNAs, and one mRNA that were dysregulated in NPC. Cellular functions of the abnormally expressed mRNAs were mainly associated with tumor cell movement, cell growth and proliferation, cell cycle, invasion, and metastasis.

**Conclusions:** The ceRNA network constructed herein clarified the regulatory mechanisms through which lncRNAs act as ceRNAs and participate in NPC development. Notably, lncRNAs, miRNAs, and mRNAs identified in this ceRNA network can serve as therapeutic targets and prognostic biomarkers for NPC.

**Keywords:** Nasopharyngeal carcinoma (NPC); long non-coding RNA (lncRNA); microRNA (miRNA); competing endogenous RNA (ceRNA); prognosis

Submitted Feb 19, 2024. Accepted for publication Jun 21, 2024. Published online Aug 08, 2024.

doi: 10.21037/tcr-24-263

View this article at: <https://dx.doi.org/10.21037/tcr-24-263>

## Introduction

Nasopharyngeal carcinoma (NPC) originates from the epithelial cells of the nasopharynx and is classified as an epithelial cancer (1). In 2020, approximately 133,354 new cases of NPC were reported globally, accounting for 0.7% of all cancer cases. In addition, there were 80,008 deaths related to NPC, accounting for 0.8% of all cancer-related deaths (2). NPC is prevalent in several regions of East and Southeast Asia, particularly in Southern China, including Guangxi and Guangdong (3). According to data from 2020, the incidence of NPC in Guangxi was 10.71 per 100,000, with a mortality rate of 5.15 per 100,000 (4).

Owing to its particular anatomical location and high response to radiation, NPC is mainly treated by radiotherapy and chemotherapy. The treatment of NPC has been improved by the development of advanced radiotherapy, concurrent chemotherapy, and precise cancer staging systems (5). However, the outlook for patients diagnosed with metastatic NPC remains unfavorable, with recurrence rates as high as 82%, even after treatment with combined radiotherapy and chemotherapy (6). Therefore, it is imperative to study the mechanisms involved in the progression of NPC to improve treatment strategies for this disease.

Bioinformatics analysis of microarray gene expression data facilitates identification of dysregulated genes and provides insights into the biological processes (BPs) involved in disease development (7). For example, Li and Zhang discovered *LINC01385*, a new long non-coding RNA (lncRNA; non-coding RNA molecules with a length exceeding 200 nucleotides) implicated in the development of NPC. Functional analysis revealed that *LINC01385* is

a potential target for therapeutic intervention in NPC (8). It has been suggested that lncRNA *H19* controls the expression of *EZH2* by interacting with *miR-630* and enhances cell invasion in NPC (9). In contrast, lncRNA *FAM225A* was found to promote NPC tumorigenesis by absorbing *miR-590-3p/miR-1275* and increasing *ITGB3* expression (10). Earlier studies have significant shortcomings because they focus on exploring the functions of only one lncRNA-microRNA (miRNA)-messenger RNA (mRNA) pathway. Therefore, our understanding of the exact molecular mechanisms and BPs underlying NPC remains limited.

Salmena *et al.* introduced the competing endogenous RNA (ceRNA) hypothesis in 2011 (11), which has been supported by various lines of evidence (12-14). They point out that any RNA transcript containing miRNA recognition elements (MREs) can compete with other transcripts that have the same MREs, leading to the sequestration of miRNAs and consequent alteration of miRNA target gene expression. To date, no specific ceRNA network has been described for NPC. Thus, it is of utmost importance to explore the impact of ceRNA networks on the unfavorable NPC prognosis. Understanding the roles of lncRNAs in NPC development may provide solutions to the most critical hurdles in managing this disease.

In this study, we aimed to utilize the Gene Expression Omnibus (GEO) database to acquire mRNA, miRNA, and lncRNA expression profiles in NPC-affected and normal tissues and perform a comprehensive analysis to construct a ceRNA network specific to NPC (a flow diagram of the study is shown in *Figure 1*). This study provides valuable insights regarding therapeutic targets for NPC, the manipulation of which could prolong patient survival, and lay the foundation for better understanding of the mechanisms underlying NPC development. We present this article in accordance with the MDAR reporting checklist (available at <https://tc.amegroups.com/article/view/10.21037/tcr-24-263/rc>).

## Methods

### Data downloading and preprocessing

We downloaded the data from the GEO database (<https://www.ncbi.nlm.nih.gov/geo/>), a reliable source of NPC gene expression profiles, using R software package GEO query (version 4.0.3, <http://r-project.org/>) (15). The mRNA expression profiles were obtained from GSE12452 (16) and

### Highlight box

#### Key findings

- We have identified key biomarkers for nasopharyngeal carcinoma (NPC) through the integration of multi-omics data.

#### What is known and what is new?

- Some long non-coding RNA have a close association with NPC.
- This is the first application of the competing endogenous RNA network in NPC.

#### What is the implication, and what should change now?

- Our study provides a direction for subsequent basic validation and clinical testing of novel NPC treatments, which could allow us to perform more targeted scientific trials.

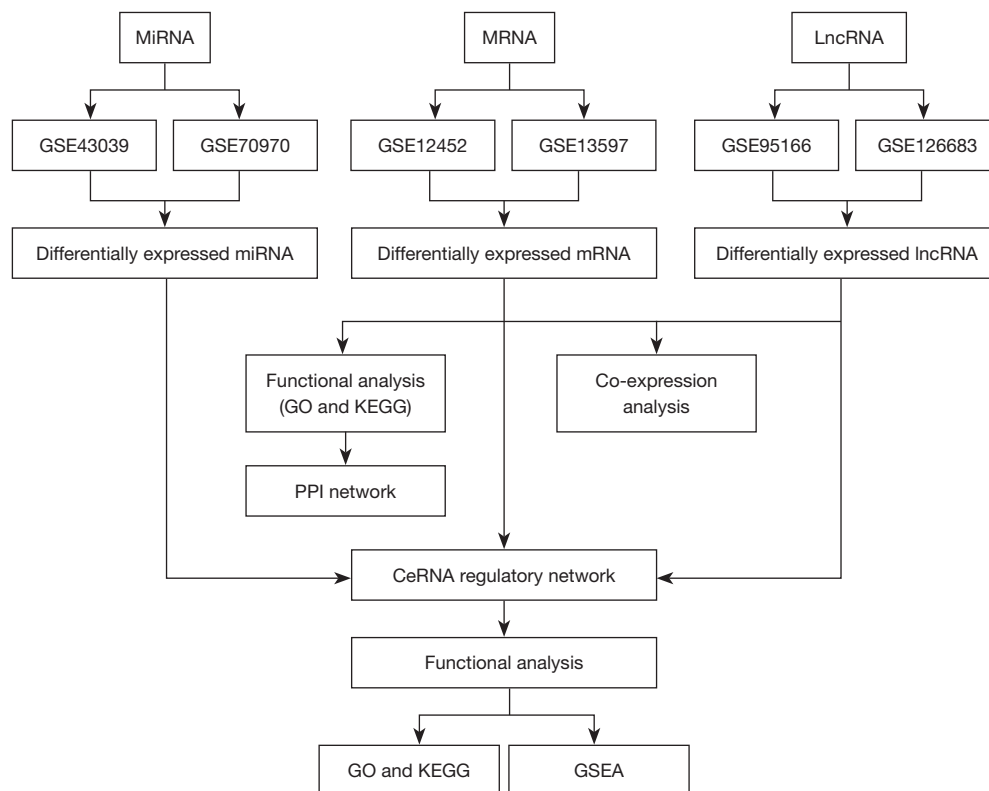


**Figure 1** The flow chart of the whole research process. MiRNA, microRNA; mRNA, messenger RNA; lncRNA, long non-coding RNA; GO, Gene Ontology; KEGG, Kyoto Encyclopedia of Genes and Genomes; PPI, protein-protein interaction; ceRNA, competing endogenous RNA; GSEA, gene set enrichment analysis.

GSE13597 (17); miRNA expression profiles were obtained from GSE43039 (18) and GSE70970 (19); and lncRNA expression profiles were derived from GSE95166 (20) and GSE126683 (10). The sample and platform information for each dataset is listed in *Table 1*. All samples were analyzed using the limma package (21) for standardized data processing. The study was conducted in accordance with the Declaration of Helsinki (as revised in 2013).

### Screening of differentially expressed genes (DEGs)

The limma package was used to identify mRNAs, miRNAs, and lncRNAs that were differentially expressed in tumor and normal samples from various datasets by using the following criteria: mRNAs,  $|\log_2\text{fold change (FC)}| > 1$ ; miRNAs,  $|\log_2\text{FC}| > 0.5$ ; lncRNAs,  $|\log_2\text{FC}| > 0.5$  ( $P < 0.05$  in all cases). Subsequently, the intersection of differentially expressed mRNA, miRNAs, and lncRNAs was performed to obtain more accurate results. The results of the analysis of DEGs were presented using heat, volcano, and Circos

maps to show the chromosomal position of DEGs and correlations of their expression levels.

### Functional analysis of differentially expressed mRNAs

Functional annotation analysis using Gene Ontology (GO) is a widely employed technique for conducting extensive studies on gene functional enrichment, encompassing molecular function (MF), BP, and cellular component (CC) (22). The Kyoto Encyclopedia of Genes and Genomes (KEGG) is a widely used database that contains comprehensive information on genomes, biological pathways, diseases, and drugs (23). The clusterProfiler package was used for GO and KEGG enrichment analyses of DEGs and effects were considered statistically significant if the adjusted P value  $< 0.05$ . In addition, this package was used to further analyze the GO and KEGG enrichment of key mRNA molecules in the ceRNA network and predict the potential regulatory functions of ceRNA networks.

**Table 1** The dataset used in this study

Type	ID	Platform	Sample	Experiment type
MRNA	GSE12452	GPL570	41	Expression profiling by array
	GSE13597	GPL96	28	Expression profiling by array
MiRNA	GSE70970	GPL20699	263	Non-coding RNA profiling by array
	GSE43039	GPL16414	40	Non-coding RNA profiling by array
LncRNA	GSE126683	GPL16956	6	Non-coding RNA profiling by array
	GSE95166	GPL15314	8	Non-coding RNA profiling by array

MRNA, messenger RNA; miRNA, microRNA; lncRNA, long non-coding RNA.

### **Construction of the protein-protein interaction (PPI) network**

The PPI network analysis of the differentially expressed RNAs was conducted using the STRING database. Cytoscape is an open-source bioinformatics software that facilitates visualization of molecular interaction networks (24). We visualized the PPI network and hub genes using Cytoscape (ver. 3.8.0) and CytoHubba plug-in (25). Hub genes were screened according to the maximum correlation standard.

### **ceRNA regulatory network construction and functional analysis**

To delve deeper into the potential correlations between mRNAs and different types of ncRNAs, a ceRNA regulatory network was created. First, to predict the interactions between miRNAs and mRNAs, we used TargetScan (<http://www.targetscan.org>) (26), miRTarBase (<https://mirtarbase.cuhk.edu.cn/>) (27), and miRDB (<http://www.mirdb.org/>) (28). The interaction between lncRNA and miRNA was predicted using the miRcode tool (<http://www.mircode.org/>), which is an extensive resource of putative miRNA target sites in the long non-coding transcriptome (29). Cytoscape 3.8.0 software was utilized to construct and visualize the ceRNA network and its core network to build and display the lncRNA-miRNA-mRNA network (25). The ggplot2 package was used to generate a Sankey diagram that visualized the regulatory relationships between lncRNAs, miRNAs, and mRNA.

### **Gene set enrichment analysis (GSEA)**

To determine the impact of a predefined set of genes on the phenotype, the GSEA was used to evaluate their

distribution trend in the order of phenotypic relevance (30). Using the GSEA, we examined the pathways and employed clusterProfiler to identify each operational cluster (31). Our cut-off thresholds included a false discovery rate <0.1 and  $P < 0.05$ .

### **Cell culture**

The NPC cell line C666 and nasopharyngeal epithelial cell line NP69 (Guangxi Medical University, Nanning, China) were cultured in RPMI-1640 medium (Asia-Vector, Shanghai, China) containing 10% fetal bovine serum (Asia-Vector) and 1% penicillin/streptomycin (Asia-Vector). The cells were cultured in an incubator at 37 °C in an atmosphere of 95% air and 5% CO<sub>2</sub>. After adherent growth was achieved, trypsin was used to detach the cells. Only cells in the logarithmic growth phase were chosen for further analysis.

### **Quantitative real-time polymerase chain reaction (qRT-PCR)**

RNA was extracted according to the TRIzol reagent protocol (Invitrogen, Carlsbad, CA, USA) and reverse-transcribed into complementary DNA (cDNA) using the Fast Quant RT Kit (TaKaRa, Otsu, Shiga, Japan). This cDNA served as template for the qRT-PCR, which was performed using the Roche Light Cycler<sup>®</sup> 480 System and Light Cycler<sup>®</sup> 480 SYBR Green I Master Mix (Roche, Pleasanton, CA, USA). The experimental data were normalized to the expression level of the *GAPDH* gene and presented as  $2^{-\Delta\Delta Ct}$  values. The primer information is shown in *Table 2*.

### **Cell transfection**

Small interfering RNAs (siRNAs) to knockdown lncRNAs

**Table 2** Primer information

RNA	Forward	Reverse
ENST00000478301	5'-GCAGAAACATCTGGTCGGTT-3'	5'-CCATTCTCTCTGCTGCTCTA-3'
ENST00000451496	5'-AAGAGCTGACACAAGAGTGGA-3'	5'-ACCACCTACAGTTGTGTTCT-3'
ENST00000544214	5'-CGGGTCACACACACCTGATT-3'	5'-GGGTCCTGCGGAAGTTCATT-3'
ENST00000505694	5'-CATTCTGGTAGAGGGCGAACCC-3'	5'-GTGACCCTGCTGCCTTCAAC-3'
ENST00000544214	5'-CGGGTCACACACACCTGATT-3'	5'-GGGTCCTGCGGAAGTTCATT-3'

were synthesized by GenePharma (Suzhou, China). Once the cells reached 50–80% confluence, they were transfected with siRNA using Lipofectamine 2000 (Invitrogen) following the manufacturer's instructions.

### Cell counting kit-8 (CCK-8) assay

In 48 h after transfection, the cells were harvested using trypsin and seeded into 96-well plates at a density of 1,000 cells per well. Cell proliferation was assessed using the CCK-8 assay (Dojindo, Kumamoto, Japan) by measuring the absorbance at 450 nm at 0, 12, 24, 48, and 72 h after reseeding, according to the manufacturer's specifications.

### Statistical analysis

The experimental data were statistically analyzed using SPSS (version 26.0; IBM, Armonk, NY, USA) and GraphPad Prism 5 software (GraphPad, La Jolla, CA, USA). Differences between groups were determined using the two-tailed Student's *t*-test. Pearson's correlation analysis was used to explore the correlation between lncRNAs and miRNAs. Effects were considered statistically significant if  $P < 0.05$ .

## Results

### Data collection and preprocessing

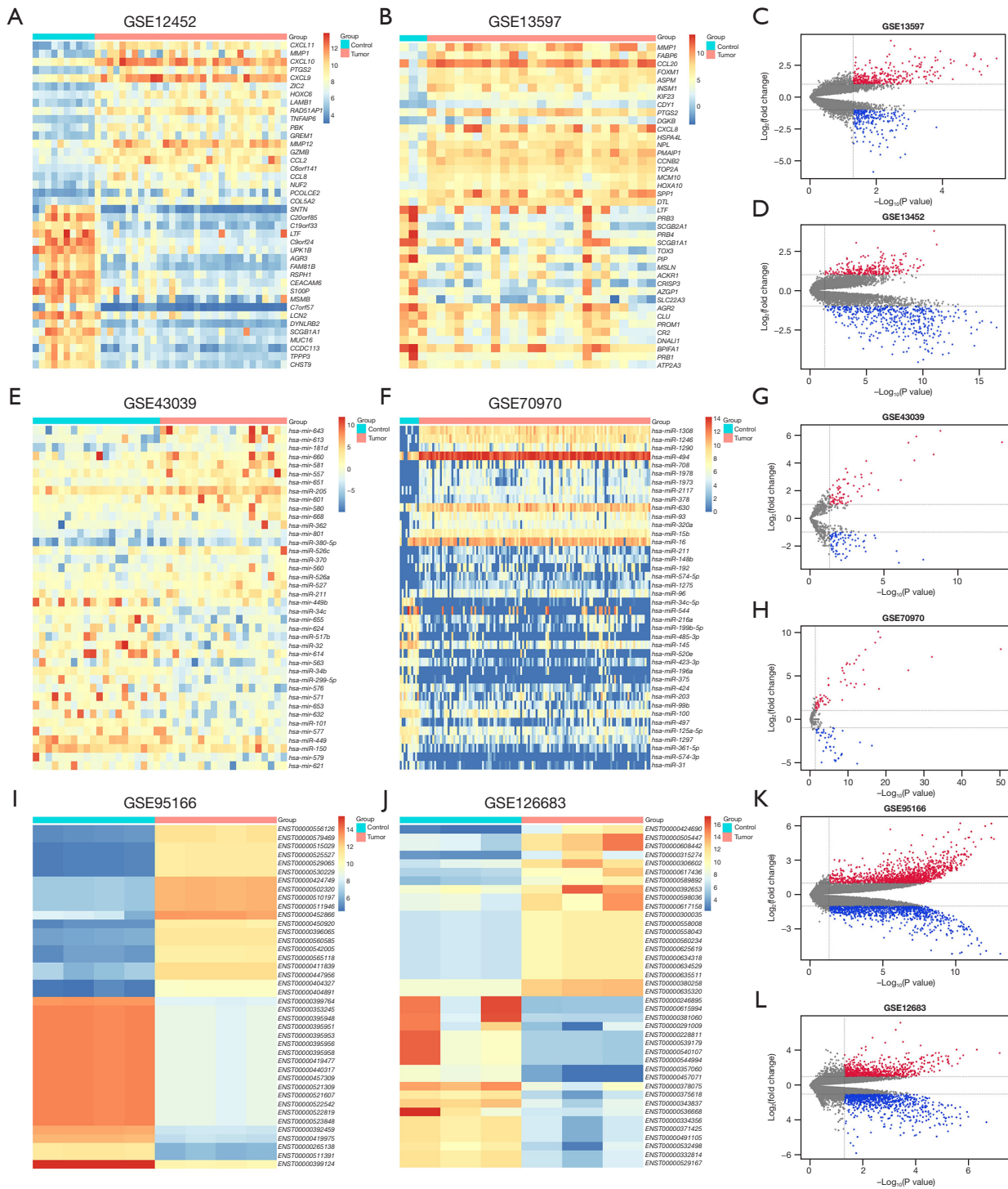
To identify DEGs in NPC samples, we used the limma package to analyze mRNA, lncRNA, and miRNA expression profiles. We found that 3,510 mRNAs, 16,520 lncRNAs, and 323 miRNAs were expressed at significantly different levels ( $|\log_2FC| \geq 1$ , adjusted  $P < 0.01$ ) in the NPC and normal tissues. Our analysis showed that dataset GSE12452 contained 2,493 differentially expressed mRNAs, including 1,265 upregulated and 1,228 downregulated mRNAs. Dataset GSE13597 contained 1,017 differentially expressed

mRNAs, including 565 upregulated and 452 downregulated mRNAs. Classification heatmaps and volcano plots of DEGs were drawn using data grouping (Figure 2A–2D). Dataset GSE43039 contained 199 differentially expressed miRNAs, including 96 upregulated and 103 downregulated molecules. A total of 124 differentially expressed miRNAs were obtained from dataset GSE70970, including 70 upregulated and 54 downregulated miRNAs (Figure 2E–2H). In dataset GSE95166, we found 9,193 differentially expressed lncRNAs, including 4,547 upregulated and 4,646 downregulated lncRNAs. In total, 7,327 differentially expressed lncRNAs were identified in dataset GSE126683, including 3,891 upregulated and 3,436 downregulated lncRNAs (Figure 2I–2L).

The overlapping differentially expressed RNA molecules are displayed using Venn diagrams (Figure 2M–2O). The chromosomal positions of the common differentially expressed mRNAs, miRNAs, and lncRNAs were determined using the RCircos package (Figure 3A–3C).

### Functional enrichment analysis

To assess the functional significance and potential BPs involving proteins encoded by mRNAs from the ceRNA network, we performed GO annotation (Figure 4A–4C) and KEGG (Figure 4D) pathway enrichment analyses. Our results revealed that the DEGs were significantly enriched in both GO and KEGG terms. Specifically, GO analysis revealed a notable enrichment of the following BPs among the DEGs: nuclear division, mitotic nuclear division, and organelle fission. The chromosomal region, chromosomes, centromeric region, and kinetochore were the most significantly enriched CCs. In addition, the following MFs were enriched: tubulin binding, microtubule binding, ATPase activity, and DNA replication origin binding. According to the KEGG pathway analysis, the dysregulated mRNAs in NPC were mainly enriched in cell



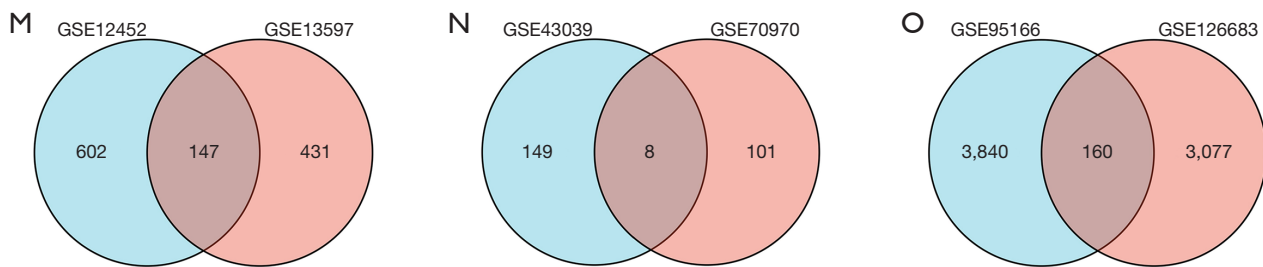


**Figure 2** Volcano plots and heatmaps show DElncRNA, DEmiRNA, and DEMRNA. Blue denotes downregulated genes, and red denotes upregulated genes. (A,B,E,F,I,J) Heatmaps for DEmiRNAs, DEMRNAs and DElncRNAs. (C,D,G,H,K,L) Volcano plots for DEmiRNAs, DEMRNAs, and DElncRNAs. (M-O) Venn diagram of differential mRNA, miRNA, and lncRNA. DElncRNA, differentially expressed long non-coding RNA; DEmiRNA, differentially expressed microRNA; DEMRNA, differentially expressed messenger RNA.

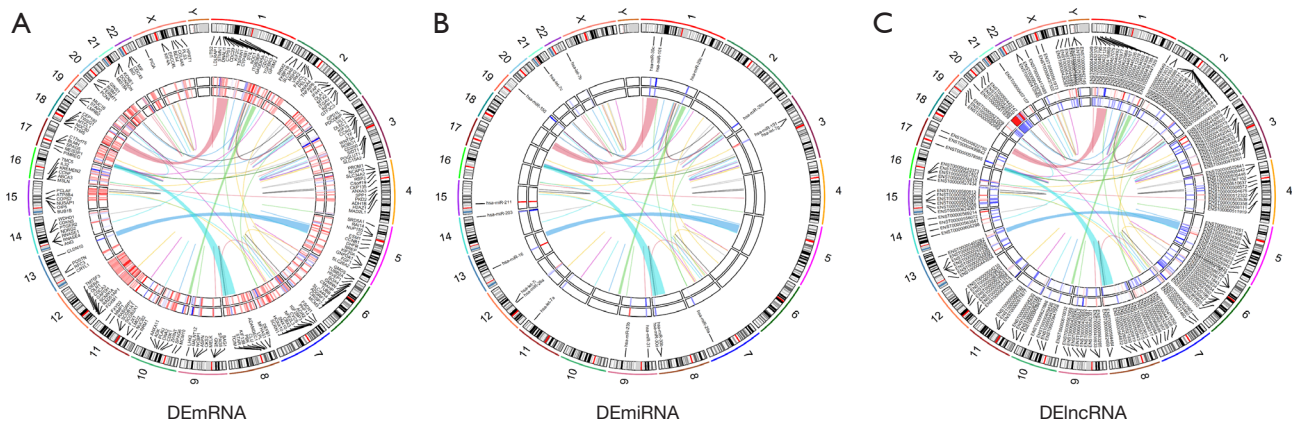


**Figure 3** Circos plot of DEMRNA (A), DEmiRNA (B), and DElncRNA (C). The outer circle shows chromosomal location information. DElncRNA, differentially expressed long non-coding RNA; DEmiRNA, differentially expressed microRNA; DEMRNA, differentially expressed messenger RNA.

cycle regulation, DNA replication, and the p53 signaling pathway. A GO functional interaction network of the differentially expressed mRNAs was constructed (Figure 4E). These findings imply that chromosomal abnormalities may have a crucial impact on NPC progression.

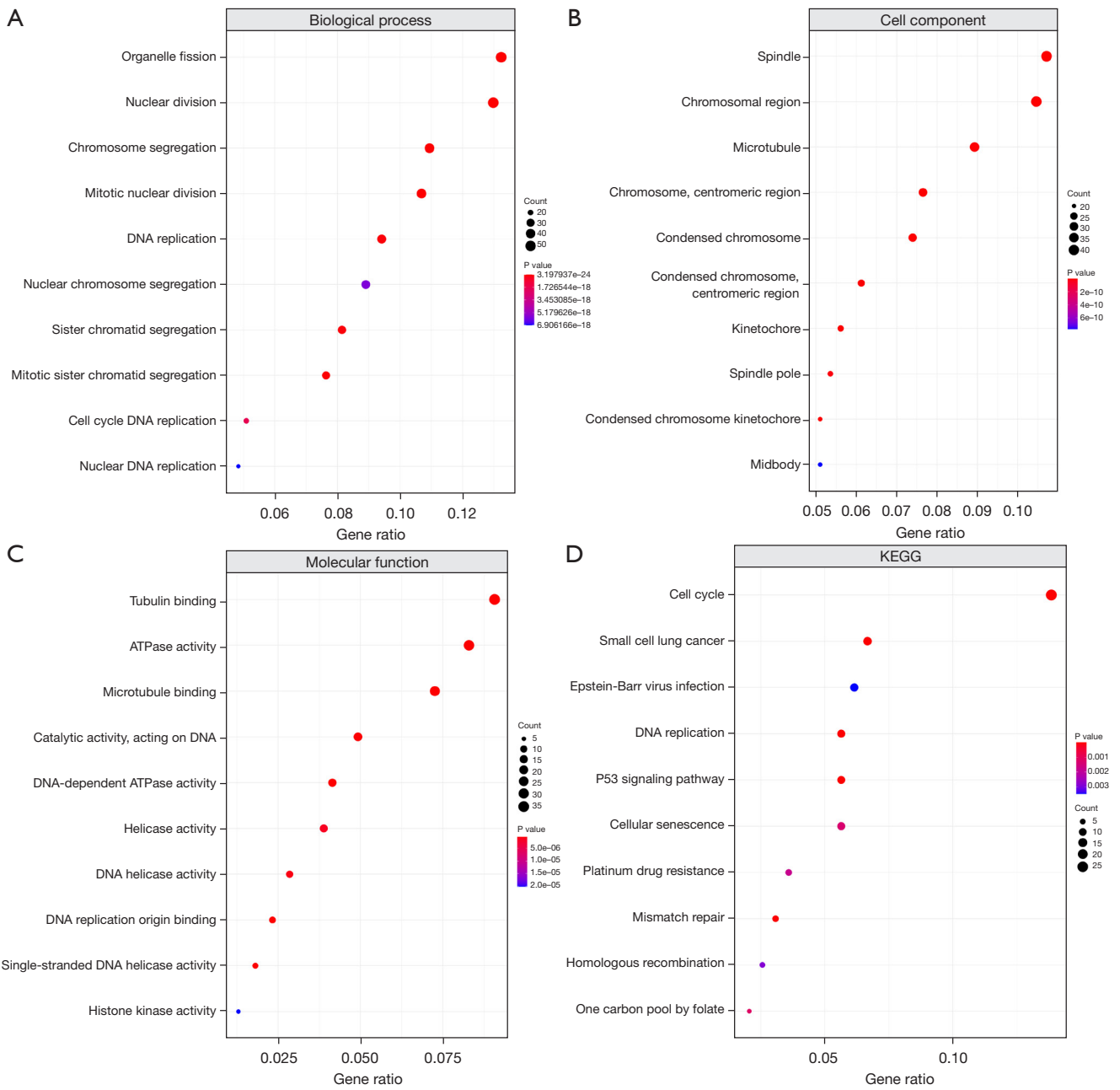
#### PPI network construction

To gain a deeper understanding of the interactions between mRNAs dysregulated in NPC, a PPI network was constructed using Cytoscape, which consisted of 146 nodes and 1,345 edges (Figure 5A). The distribution of node degrees in the PPI network was analyzed, and the top 30 mRNAs with the highest degrees are shown in Figure 5B. The mRNAs of the top 10 hub genes (*CDK1*, *CDC20*, *NUSAP1*, *KIF11*, *KIF20A*, *DLGAP5*, *CCNA2*, *BUB1B*,

*TOP2A*, and *ASPM*) were screened from the differentially expressed mRNAs (Figure 5C). These genes may aid in exploration of the biological mechanisms underlying NPC development and reveal potential therapeutic targets.

#### ceRNA network construction and lncRNA-mRNA co-expression analysis

To investigate the roles of various types of RNA in NPC, we analyzed correlations between lncRNA and mRNA expression levels as well as correlations between expression levels of miRNAs and those of their corresponding target mRNAs and lncRNAs (Figure 6A,6B). We found that lncRNAs such as *ENST00000220514* and *ENST00000301633* were significantly positively correlated with mRNAs, whereas *ENST000000330915* and





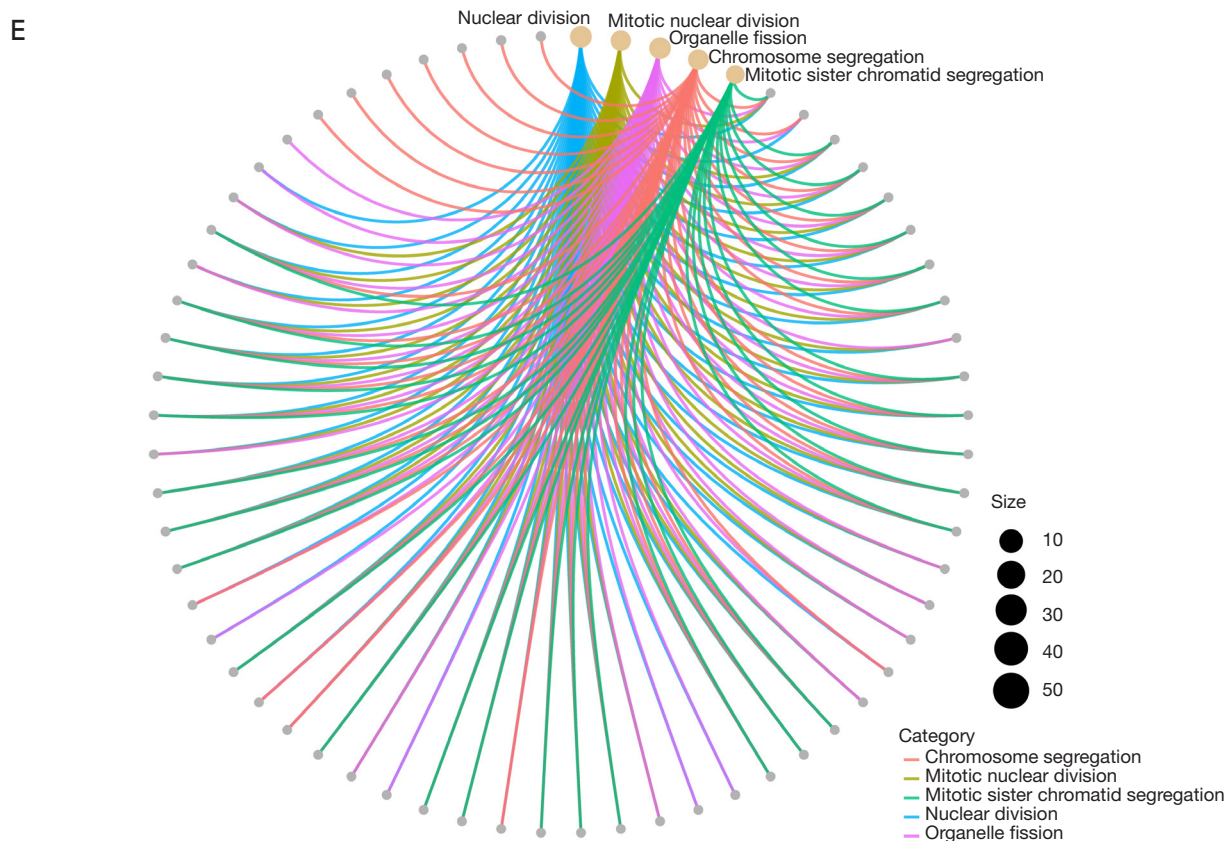


**Figure 4** GO and KEGG pathway enrichment analysis of DEmRNA. (A) Bubble plot of BP. (B) Bubble plot of CC. (C) Bubble plot of MF. (D) Bubble plot of KEGG. (E) The network shows the GO enrichment analysis results and the gene interaction in GO term. Size represents the number of genes enriched; category represents the function term. KEGG, Kyoto Encyclopedia of Genes and Genomes; GO, Gene Ontology; DEmRNA, differentially expressed messenger RNA; BP, biological process; CC, cell component; MF, molecular function.

*ENST00000332503* were significantly negatively correlated with mRNAs. Based on the expression profiles of the differentially expressed miRNAs, lncRNAs, and mRNAs in patients with NPC, we constructed a ceRNA network consisting of 7 miRNA nodes, 18 mRNA nodes, and 10 lncRNA nodes. Furthermore, we evaluated the topological significance of each gene within the ceRNA network by calculating its degree of connectivity (Figure 7A, 7B).

#### *ceRNA core module screening and functional analysis*

By applying the degree and maximum correlation standard algorithm in CytoHubba, we discovered five hub miRNAs, four lncRNAs, and one mRNA as a core module (Figure 8A). The ceRNA regulatory network suggested that *CCNE2* may play a key role as an effector. Biological analyses were performed using clusterProfiler to examine *CCNE2*

protein functions. We found that *CCNE2* is significantly enriched in both GO and KEGG terms (Figure 8B, 8C). GO analysis revealed that *CCNE2* mRNA was notably enriched in BPs such as fungiform papillary morphogenesis, tongue morphogenesis, and ectodermal placode formation. According to the KEGG analysis, *CCNE2* demonstrated significant enrichment in various pathways, such as the cell cycle, neutrophil extracellular trap formation, and transcriptional misregulation in cancer. We then explored potential regulatory pathways using GSEA and found that the results of GSEA were also mainly related to cell cycle-related functions (Figure 8D–8M).

#### *ENST00000451496 was highly expressed in C666 cells and required for their proliferation*

To validate expression profiles of five lncRNAs in NPC

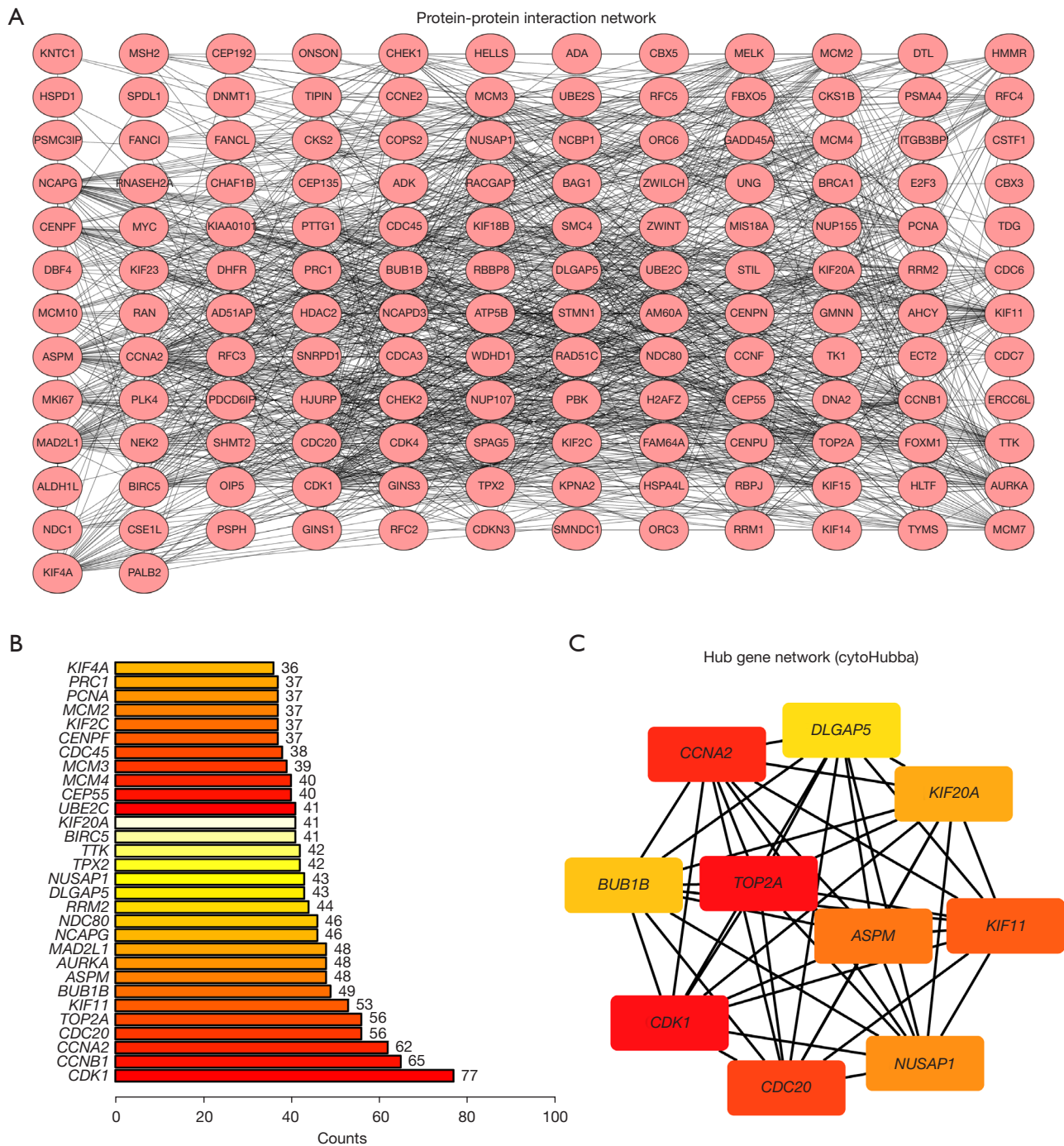


**Figure 5** PPI network and hub gene analysis. (A) PPI network of DEmRNA. (B) The degree distribution of the PPI network of the top 30 NPC specific mRNAs. (C) Hub-genes in the PPI network. The redder the color, the higher the ranking. PPI, protein-protein interaction; DEmRNA, differentially expressed messenger RNA; NPC, nasopharyngeal carcinoma; mRNA, messenger RNA.



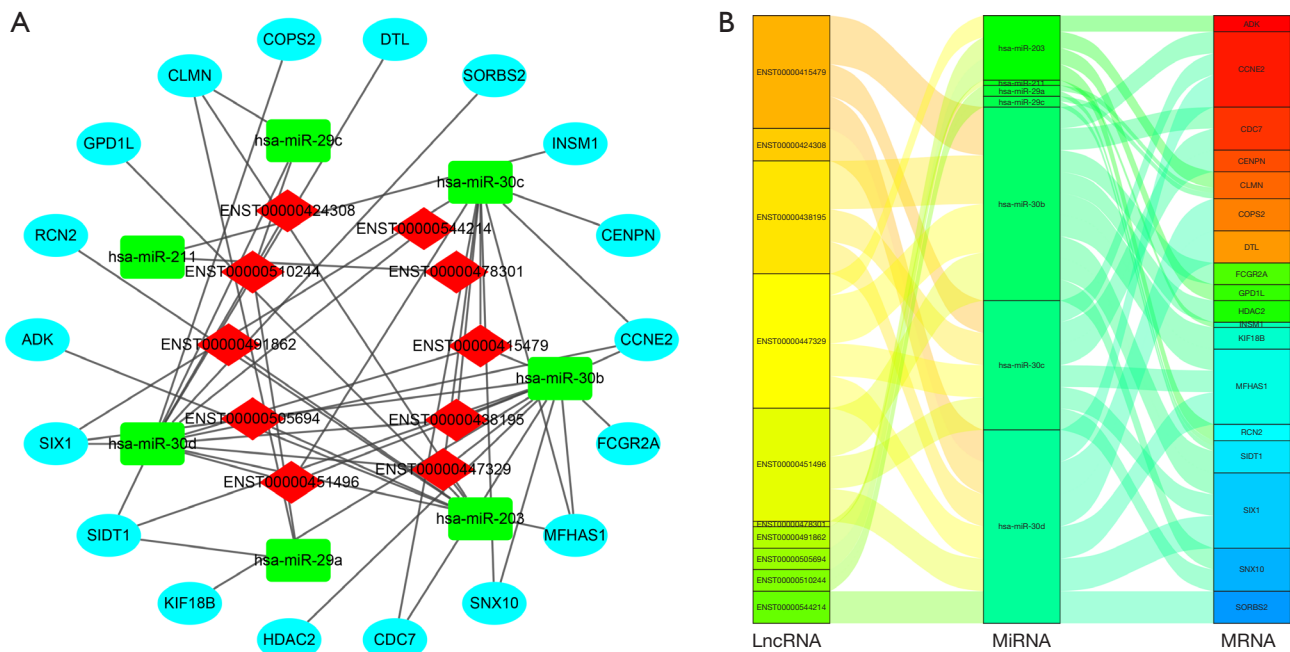


**Figure 7** Construction of ceRNA network in NPC. (A) LncRNA-miRNA-mRNA ceRNA network. The rectangles indicate miRNAs in green, ellipses represent mRNAs in light blue and diamonds represent lncRNAs in red. (B) Sankey diagram for the ceRNA network in NPC. Each rectangle represents a gene, and the connection degree of each gene is visualized based on the size of the rectangle. LncRNA, long non-coding RNA; miRNA, microRNA; mRNA, messenger RNA; ceRNA, competing endogenous RNA; NPC, nasopharyngeal carcinoma.

cells, qRT-PCR was performed in C666 and NP69 cells. The C666 cells had elevated expression levels of *ENST00000478301* and *ENST00000451496*, whereas lncRNAs *ENST00000510244*, *ENST00000505694*, and *ENST00000544214* were expressed at relatively lower levels in the C666 cells compared to those in the NP69 cells. These findings suggest potential roles for *ENST00000478301* and *ENST00000451496* in NPC pathogenesis and warrant further investigation of their molecular mechanisms of action. To further elucidate the functional roles of these two lncRNAs, the C666 cells were transfected with corresponding siRNAs and a negative control siRNA. qPCR analysis revealed that *ENST00000451496*-siRNA1/4 and *ENST00000478301*-siRNA-3/4 had superior efficacy and were therefore selected for subsequent experiments. The CCK-8 assay indicated that *ENST00000451496* knockdown led to a more pronounced inhibition of C666 cell proliferation compared to that afforded by *ENST00000478301* knockdown at 12, 24, 48, and 72 h post-treatment, prompting us to focus on *ENST00000451496* in the subsequent analysis (Figure 9).

### Discussion

NPC is a malignant tumor of the head and neck, and the resistance to treatment of NPC distant metastases is the major cause of patient mortality. Despite the adoption of various treatment strategies, such as radiation therapy and chemotherapy, the prognosis of NPC patients who receive these treatments remains unsatisfactory (32). Understanding the molecular mechanisms and processes that contribute to NPC is crucial for identifying novel therapeutic targets and improving clinical outcomes of patients with this disease. According to the ceRNA hypothesis, lncRNAs are considered miRNA sponges because of their ability to bind and neutralize miRNAs, thereby having a regulatory impact (33,34). Therefore, a comprehensive understanding of lncRNA-miRNA-mRNA interactions will enhance our understanding of the onset and progression of NPC.

In this study, we identified 3,510 mRNAs, 16,520 lncRNAs, and 323 miRNAs that were differentially expressed in patients with NPC. We then used these DEGs to establish a ceRNA network linked to lncRNAs, enabling

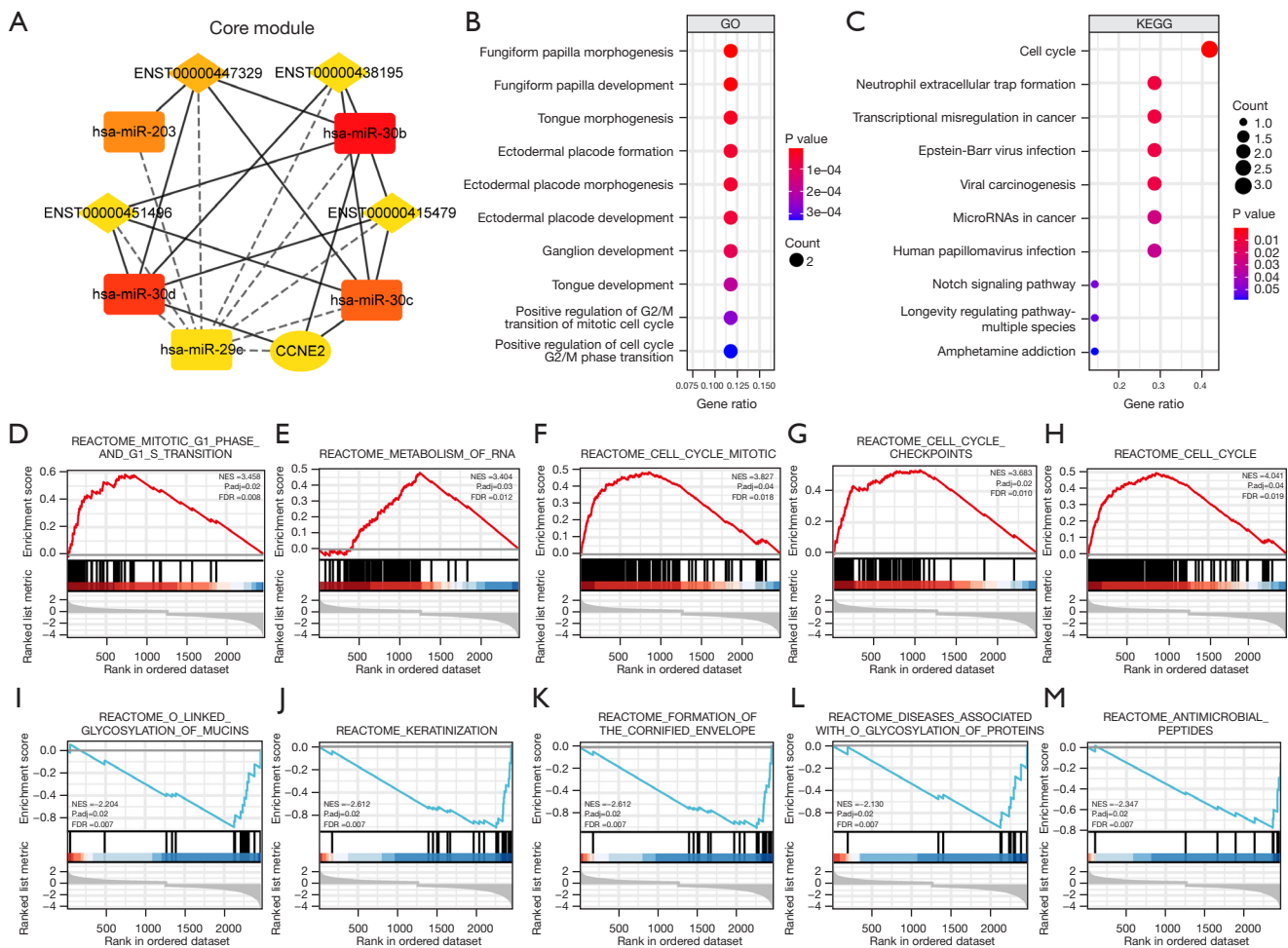


**Figure 8** The sub-network of ceRNA and functional analysis. (A) CytoHubba was used to screen ceRNA core genes. The red rectangle, orange diamond, and yellow oval represent miRNA, lncRNA, and mRNA respectively. (B) GO functional enrichment analysis results. (C) KEGG pathway enrichment analysis results. (D-H) GSEA results of the top 5 upregulated signaling pathway. (I-M) GSEA results of the top 5 downregulated signaling pathway. The X-coordinate is the gene ratio, and the Y-coordinate is the pathway result. Red and blue colors represent up and downregulation respectively. NES value represents the enrichment value after normalization, and a larger NES value means more genes enriched in this pathway. The P value reflects the reliability of the enrichment results. GO, Gene Ontology; KEGG, Kyoto Encyclopedia of Genes and Genomes; ceRNA, competing endogenous RNA; miRNA, microRNA; lncRNA, long non-coding RNA; mRNA, messenger RNA; GSEA, gene set enrichment analysis; NES, normalized enrichment score.

us to investigate the regulatory mechanisms of ceRNAs. This ceRNA network included 20 lncRNAs, 30 miRNAs, and 30 mRNAs that were differentially expressed specifically in NPC. Among them, four lncRNAs (*ENST00000438195*, *ENST00000415479*, *ENST00000451496*, and *ENST00000447329*), one mRNA (*CCNE2*) and five miRNAs (*hsa-miR-203*, *hsa-miR-30b*, *hsa-miR-30d*, *hsa-miR-30c*, and *hsa-miR-29c*) were identified as hub genes. Among the prognostic differentially expressed lncRNAs

in the ceRNA network, the lncRNA *ENST00000447329* (also known as *LINC01358*) has the highest degree of connectivity (5). Thus, we concluded that it could have a significant impact on NPC pathogenesis. In the hub miRNAs, *hsa-miR-29c* plays a crucial role in NPC. *In vitro* experiments showed that the overexpression of *hsa-miR-29c* inhibited the migration and invasion of NPC cells (35). Decreased *miR-29c* expression is associated with increased resistance to therapy in patients with NPC. This is because

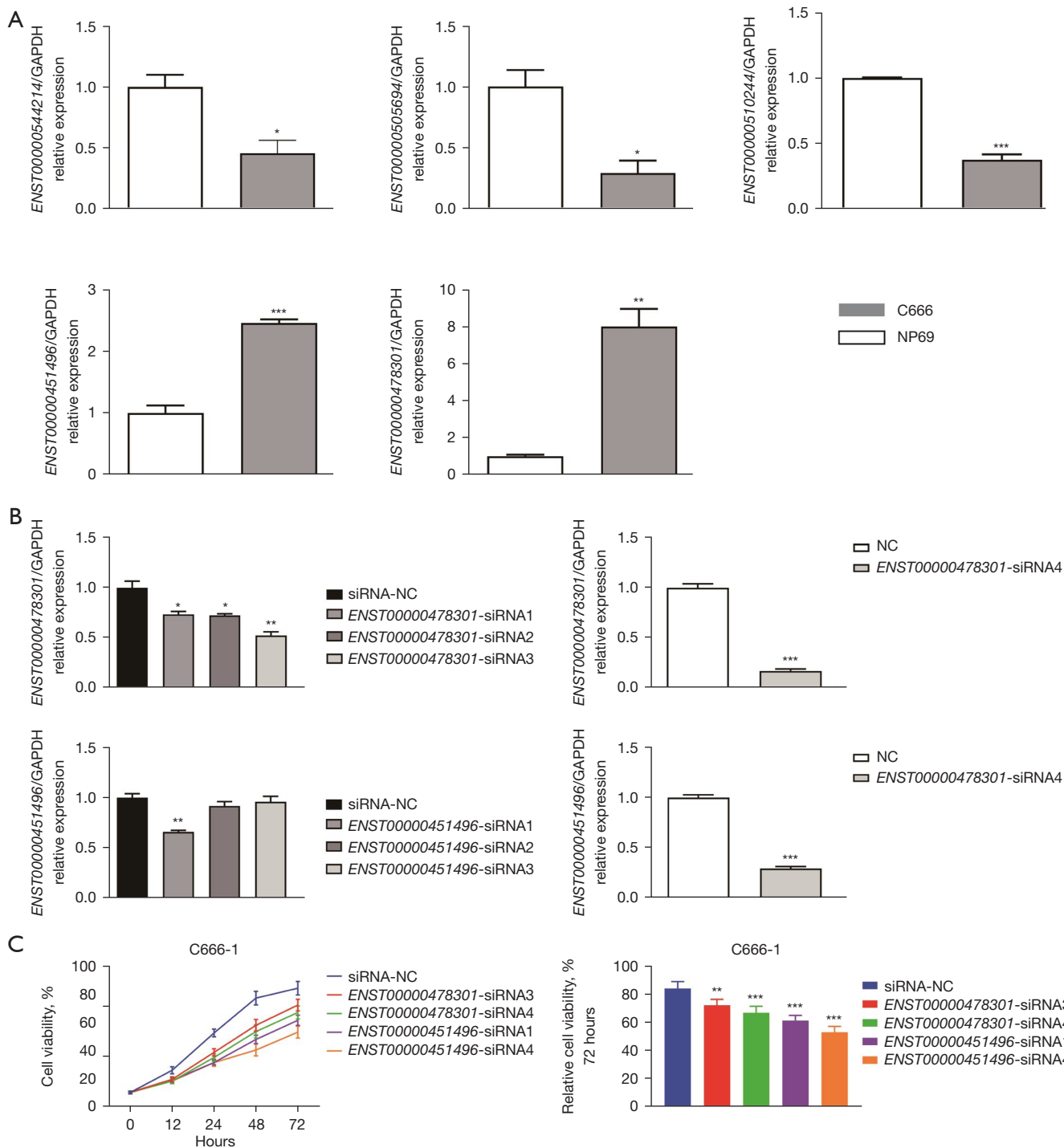


**Figure 9** Analysis of lncRNAs in C666 cell lines and NP69 cell lines. (A) Results of qRT-PCR in different cell lines for five lncRNAs. *ENST00000478301* and *ENST00000451496* were significantly upregulated in NPC cell line C666. (B) *ENST00000451496*-siRNA1/4 and *ENST00000478301*-siRNA-3/4 had superior knockdown efficacy. (C) The proliferation ability of C666 cells transfected with NC or *ENST00000478301* or *ENST00000451496* was examined by CCK-8 assay. Knockdown *ENST00000451496* led to a more pronounced inhibition of C666 cell proliferation. \*, P<0.05; \*\*, P<0.01; \*\*\*, P<0.001. siRNA, small interfering RNA; NC, negative control; lncRNA, long non-coding RNA; qRT-PCR, quantitative real-time polymerase chain reaction; NPC, nasopharyngeal carcinoma; CCK-8, cell counting kit-8.

*miR-29c* inhibits expression of the anti-apoptotic factors Mcl-1 and Bcl-2, leading to an increased sensitivity of NPC cells to ionizing radiation and cisplatin treatment (36). Additionally, according to Yu *et al.*, the upregulation of *miR-203* inhibits the G1/S transition in cells infected with Epstein-Barr virus and hinders tumor growth *in vivo*, suggesting that *miR-203* could serve as a potential biomarker for the diagnosis and treatment of Epstein-Barr virus-associated NPC (37). Based on our findings, we hypothesized that the *hsa-miR-203* and *hsa-miR-29c* axes play significant roles in the development of NPC and could serve as promising targets for therapeutic interventions in this cancer.

Among the prognostic DEGs, *CCNE2* has the highest degree of connectivity (4) among other differentially expressed mRNAs. *CCNE2* binds to and activates CDK2, forming a kinase complex that participates in the G1/S phase transition, thereby regulating cell proliferation and tumor development (38-40). According to a study by Xie *et al.* performed on 308 samples of ovarian cancer tissues, high *CCNE2* expression is linked to reduced overall survival (41). Similarly, a study of prostate cancer has indicated that *CCNE2* is substantially upregulated in patients with this condition and is regarded as a protein that promotes tumor growth (42). Our GO analysis showed that differentially expressed mRNAs were mainly associated with the morphogenesis of the fungiform papilla, tongue, and ectodermal placode. The KEGG pathway analysis demonstrated that the differentially expressed mRNAs were significantly enriched in several pathways, including the cell cycle, formation of neutrophil extracellular traps, transcriptional misregulation in cancer, Epstein-Barr virus infection, and viral carcinogenesis, which are all closely associated with cancer development. This finding not only indicates the reliability of the constructed ceRNA regulatory network but also supports the necessity of studying lncRNAs as ceRNA regulators, which could serve as therapeutic targets in NPC.

Although we developed an NPC-specific ceRNA regulatory network and identified potential prognostic biomarkers, our study had several limitations. First, we relied solely on gene expression data obtained from the GEO database. Further prospective studies involving larger patient populations from different centers are required to validate our results. Second, the bioinformatics analysis results require extensive experimental verification before they can be implemented in clinical practice. Future research should focus on the functional and mechanistic

validation of genes dysregulated in NPC to ensure practical application of our findings.

## Conclusions

In this study, we constructed a novel ceRNA network that provided several mechanistic clues regarding the interactions between genes dysregulated in NPC. Our results not only provide theoretical support for revealing the regulatory relationship between lncRNAs, miRNAs, and mRNAs in NPC but also offer a more substantiated approach for exploring clinical diagnostic markers and potential therapeutic targets in NPC. Furthermore, our study provides a direction for subsequent basic validation and clinical testing of novel NPC treatments, which could allow us to perform more targeted scientific trials, thereby sparing valuable research resources.

## Acknowledgments

**Funding:** This work was supported by the National Natural Science Foundation of China (No. 82260627).

## Footnote

**Reporting Checklist:** The authors have completed the MDAR reporting checklist. Available at <https://tcr.amegroups.com/article/view/10.21037/tcr-24-263/rc>

**Data Sharing Statement:** Available at <https://tcr.amegroups.com/article/view/10.21037/tcr-24-263/dss>

**Peer Review File:** Available at <https://tcr.amegroups.com/article/view/10.21037/tcr-24-263/prf>

**Conflicts of Interest:** All authors have completed the ICMJE uniform disclosure form (available at <https://tcr.amegroups.com/article/view/10.21037/tcr-24-263/coif>). The authors have no conflicts of interest to declare.

**Ethical Statement:** The authors are accountable for all aspects of the work in ensuring that questions related to the accuracy or integrity of any part of the work are appropriately investigated and resolved. This study was conducted in accordance with the Declaration of Helsinki (as revised in 2013).

**Open Access Statement:** This is an Open Access article

distributed in accordance with the Creative Commons Attribution-NonCommercial-NoDerivs 4.0 International License (CC BY-NC-ND 4.0), which permits the non-commercial replication and distribution of the article with the strict proviso that no changes or edits are made and the original work is properly cited (including links to both the formal publication through the relevant DOI and the license). See: <https://creativecommons.org/licenses/by-nc-nd/4.0/>.

## References

1. Chua MLK, Wee JTS, Hui EP, et al. Nasopharyngeal carcinoma. *Lancet* 2016;387:1012-24.
2. Sung H, Ferlay J, Siegel RL, et al. Global Cancer Statistics 2020: GLOBOCAN Estimates of Incidence and Mortality Worldwide for 36 Cancers in 185 Countries. *CA Cancer J Clin* 2021;71:209-49.
3. Chang ET, Ye W, Zeng YX, et al. The Evolving Epidemiology of Nasopharyngeal Carcinoma. *Cancer Epidemiol Biomarkers Prev* 2021;30:1035-47.
4. Niu Y, Zhang F, Chen D, et al. A comparison of Chinese multicenter breast cancer database and SEER database. *Sci Rep* 2022;12:10395.
5. Chen YP, Chan ATC, Le QT, et al. Nasopharyngeal carcinoma. *Lancet* 2019;394:64-80.
6. Prawira A, Oosting SF, Chen TW, et al. Systemic therapies for recurrent or metastatic nasopharyngeal carcinoma: a systematic review. *Br J Cancer* 2017;117:1743-52.
7. Behzadi P, Ranjbar R. DNA microarray technology and bioinformatic web services. *Acta Microbiol Immunol Hung* 2019;66:19-30.
8. Li L, Zhang F. Novel long noncoding RNA LINC01385 promotes nasopharyngeal carcinoma proliferation via the miR-140-3p/Twist1 signaling pathway. *Cell Cycle* 2020;19:1352-62.
9. Ng A, Tang JP, Goh CH, et al. Regulation of the H19 imprinting gene expression in human nasopharyngeal carcinoma by methylation. *Int J Cancer* 2003;104:179-87.
10. Zheng ZQ, Li ZX, Zhou GQ, et al. Long Noncoding RNA FAM225A Promotes Nasopharyngeal Carcinoma Tumorigenesis and Metastasis by Acting as ceRNA to Sponge miR-590-3p/miR-1275 and Upregulate ITGB3. *Cancer Res* 2019;79:4612-26.
11. Salmena L, Poliseno L, Tay Y, et al. A ceRNA hypothesis: the Rosetta Stone of a hidden RNA language? *Cell* 2011;146:353-8.
12. Ebert MS, Neilson JR, Sharp PA. MicroRNA sponges: competitive inhibitors of small RNAs in mammalian cells. *Nat Methods* 2007;4:721-6.
13. Poliseno L, Salmena L, Zhang J, et al. A coding-independent function of gene and pseudogene mRNAs regulates tumour biology. *Nature* 2010;465:1033-8.
14. Wang J, Liu X, Wu H, et al. CREB up-regulates long non-coding RNA, HULC expression through interaction with microRNA-372 in liver cancer. *Nucleic Acids Res* 2010;38:5366-83.
15. Davis S, Meltzer PS. GEOquery: a bridge between the Gene Expression Omnibus (GEO) and BioConductor. *Bioinformatics* 2007;23:1846-7.
16. Dodd LE, Sengupta S, Chen IH, et al. Genes involved in DNA repair and nitrosamine metabolism and those located on chromosome 14q32 are dysregulated in nasopharyngeal carcinoma. *Cancer Epidemiol Biomarkers Prev* 2006;15:2216-25.
17. Bose S, Yap LF, Fung M, et al. The ATM tumour suppressor gene is down-regulated in EBV-associated nasopharyngeal carcinoma. *J Pathol* 2009;217:345-52.
18. Lyu X, Fang W, Cai L, et al. TGFβR2 is a major target of miR-93 in nasopharyngeal carcinoma aggressiveness. *Mol Cancer* 2014;13:51.
19. Bruce JP, Hui AB, Shi W, et al. Identification of a microRNA signature associated with risk of distant metastasis in nasopharyngeal carcinoma. *Oncotarget* 2015;6:4537-50.
20. Xu Y, Huang X, Ye W, et al. Comprehensive analysis of key genes associated with ceRNA networks in nasopharyngeal carcinoma based on bioinformatics analysis. *Cancer Cell Int* 2020;20:408.
21. Ritchie ME, Phipson B, Wu D, et al. limma powers differential expression analyses for RNA-sequencing and microarray studies. *Nucleic Acids Res* 2015;43:e47.
22. Ashburner M, Ball CA, Blake JA, et al. Gene ontology: tool for the unification of biology. The Gene Ontology Consortium. *Nat Genet* 2000;25:25-9.
23. Ogata H, Goto S, Sato K, et al. KEGG: Kyoto Encyclopedia of Genes and Genomes. *Nucleic Acids Res* 1999;27:29-34.
24. Shannon P, Markiel A, Ozier O, et al. Cytoscape: a software environment for integrated models of biomolecular interaction networks. *Genome Res* 2003;13:2498-504.
25. Assenov Y, Ramírez F, Schelhorn SE, et al. Computing topological parameters of biological networks. *Bioinformatics* 2008;24:282-4.
26. Agarwal V, Bell GW, Nam JW, et al. Predicting effective microRNA target sites in mammalian mRNAs. *Elife*



- 2015;4:e05005.
27. Huang HY, Lin YC, Li J, et al. miRTarBase 2020: updates to the experimentally validated microRNA–target interaction database. *Nucleic Acids Res* 2020;48:D148–54.
  28. Chen Y, Wang X. miRDB: an online database for prediction of functional microRNA targets. *Nucleic Acids Res* 2020;48:D127–31.
  29. Jeggari A, Marks DS, Larsson E. miRcode: a map of putative microRNA target sites in the long non-coding transcriptome. *Bioinformatics* 2012;28:2062–3.
  30. Subramanian A, Tamayo P, Mootha VK, et al. Gene set enrichment analysis: a knowledge-based approach for interpreting genome-wide expression profiles. *Proc Natl Acad Sci U S A* 2005;102:15545–50.
  31. Yu G, Wang LG, Han Y, et al. clusterProfiler: an R package for comparing biological themes among gene clusters. *OMICS* 2012;16:284–7.
  32. Lee HM, Okuda KS, González FE, et al. Current Perspectives on Nasopharyngeal Carcinoma. *Adv Exp Med Biol* 2019;1164:11–34.
  33. Tan JY, Sirey T, Honti F, et al. Extensive microRNA-mediated crosstalk between lncRNAs and mRNAs in mouse embryonic stem cells. *Genome Res* 2015;25:655–66.
  34. Duan X, Wu Y, Zhang Z, et al. Identification and analysis of dysregulated lncRNA and associated ceRNA in the pathogenesis of keloid. *Ann Transl Med* 2020;8:222.
  35. Liu N, Tang LL, Sun Y, et al. MiR-29c suppresses invasion and metastasis by targeting TIAM1 in nasopharyngeal carcinoma. *Cancer Lett* 2013;329:181–8.
  36. Zhang JX, Qian D, Wang FW, et al. MicroRNA-29c enhances the sensitivities of human nasopharyngeal carcinoma to cisplatin-based chemotherapy and radiotherapy. *Cancer Lett* 2013;329:91–8.
  37. Yu H, Lu J, Zuo L, et al. Epstein-Barr virus downregulates microRNA 203 through the oncoprotein latent membrane protein 1: a contribution to increased tumor incidence in epithelial cells. *J Virol* 2012;86:3088–99.
  38. Lauper N, Beck AR, Cariou S, et al. Cyclin E2: a novel CDK2 partner in the late G1 and S phases of the mammalian cell cycle. *Oncogene* 1998;17:2637–43.
  39. Gudas JM, Payton M, Thukral S, et al. Cyclin E2, a novel G1 cyclin that binds Cdk2 and is aberrantly expressed in human cancers. *Mol Cell Biol* 1999;19:612–22.
  40. Aleem E, Kiyokawa H, Kaldis P. Cdc2-cyclin E complexes regulate the G1/S phase transition. *Nat Cell Biol* 2005;7:831–6.
  41. Xie L, Li T, Yang LH. E2F2 induces MCM4, CCNE2 and WHSC1 upregulation in ovarian cancer and predicts poor overall survival. *Eur Rev Med Pharmacol Sci* 2017;21:2150–6.
  42. Liu B, Qian D, Zhou W, et al. A Novel Androgen-Induced lncRNA FAM83H-AS1 Promotes Prostate Cancer Progression via the miR-15a/CCNE2 Axis. *Front Oncol* 2021;10:620306.

**Cite this article as:** Li Y, Zhong H, Luo L, Gan M, Liang L, Que L, Zheng S, Zhong J, Liang L. Integrated analysis of the lncRNA-miRNA-mRNA ceRNA network in nasopharyngeal carcinoma. *Transl Cancer Res* 2024;13(8):4372–4388. doi: 10.21037/tcr-24-263